Journal of
Nanoscience and Nanotechnology
Vol. 5, 2029–2033, 2005

Packaging of Gold Particles in Viral Capsids

Chao Chen,[1] Eun-Soo Kwak,[1] Barry Stein,[2] C. Cheng Kao,[3] and Bogdan Dragnea[1,*]

[1]*Department of Chemistry, Indiana University, Bloomington, Indiana 47405, USA*
[2]*Indiana Molecular Biology Institute, Indiana University, Bloomington, Indiana 47405, USA*
[3]*Department of Biochemistry and Biophysics, Texas A&M University, College Station, Texas 77843-2128, USA*

In-vitro self-assembly conditions known to result in generating infectious virions have been used *in vitro* to reassemble bromovirus capsid proteins around negatively charged gold nanoparticles cores. We discuss here the optical properties (elastic light scattering) and the influence of the core size and of the functional moiety on the resulting virus-like particles. Our results indicate that the formation of a closed shell, as opposed to an amorphous protein coat, does occur and that the shell/core interactions can be tuned using different coatings on the nanoparticle core. Such studies may lead to real-time monitoring of viral traffic on the scale of a single virus, as well as to the possibility of chemical sensing along the intracellular and intercellular viral pathways and contribute to a better understanding of the virus transport and cellular compartmentalization.

Keywords: Virus Self-Assembly, Icosahedral, Brome Mosaic, Encapsidation, Gold Nanoparticles, Nanoprobe Microscopy, Single Virus Tracking.

RESEARCH ARTICLE

1. INTRODUCTION

Viruses have a protein coat, known as capsid, surrounding their genomic nucleic acids. From a materials point of view, viral capsids are interesting because they represent a paradigm for complex macromolecular assemblies in which the assembly process actively changes the initial building blocks.[1] Molecular switching often occurs subsequent to the association process. The molecular events associated with it include rigid subunit rotations, refolding and phase transitions of the assembled complex.[2] Such switches are responsible for the functional and ecological roles held by the capsid during viral infection and spread.[3] Understanding the capsid dynamics is particularly appealing since, to date, there are no examples of man-made single component materials that can self-assemble to gain multi-functionality.

Another appeal of virus capsids as materials is that they can be produced *in-vitro* from homologous protein solutions that can assemble upon a change in the buffer environment.[4] Their highly monodisperse physical and chemical properties has brought about the emergence of new examples of elegant nanoscale template chemistry.[5,6] Furthermore, nanoscale viral capsids are ideal delivery vectors, promising for specific targeting of therapeutic macromolecules[7] or for optical probes with biomedical imaging and sensing purposes having unprecedented resolution and sensitivity.[8,9] Such optical probes depend on the success of encapsulation of optically active particles inside viruses. We have recently demonstrated that single viral particles containing a gold particle core could be individually imaged and spectroscopically analyzed by light microscopy.[9] These studies used a simple icosahedral viral capsids surrounding a 4–5 nm diameter core of citrate-functionalized, negatively charged gold nanoparticle. In this paper, we extend the studies of virus-encapsulated nanoparticles to show that the protein coat forms an intact, closed shell around the nanoparticle core. Moreover, the size of the encapsidated particle does not interfere with the size of the surrounding shell. However, the charged moieties on the nanoparticle have an important role in determining the radius of curvature of the complex. In other words, it seems that according to the nature of the moieties on the nanoparticle surface one can toggle the capsid between two states of aggregation. When DNA-coated Au particles are used, the concentration of functionalized viral particles is high enough to allow for bulk fluorescence quenching and surface plasmon spectroscopy. The fluorescence quenching properties of the Au cores have been used to demonstrate that the protein shell is compact enough to frustrate the diffusion of fluorescent dyes, which also supports the idea of a complete closed shell formation.

*Author to whom correspondence should be addressed.

1533-4880/2005/5/2029/005 doi:10.1166/jnn.2005.506

To date, two routes of particle entrapping inside virus capsids have been reported. Douglas and Young have utilized the formation of openings in the cowpea chlorotic mottle virus capsid during the reversible expansion induced by pH changes, which allowed for free molecular exchange and subsequent selective nucleation and growth of polyoxometalate single crystals within the virus cavity. This method, to be called the "synthesis method" here, has the advantages of maintaining the virus capsid assembled at all times and of high yields of nanoparticle entrapment. However, the range of materials that can be incorporated is limited by the compatibility between the synthetic conditions, the chemical features of the input material, and capsid stability.[5] Dragnea et al. applied a protocol adapted from the *in vitro* assembly of cowpea chlorotic mottle virus to the brome mosaic virus (BMV)[10] to associate negatively charged Au particles with the internal compartment of BMV capsids in three steps: complete disassembly of the BMV virions and purification of the capsid subunits, reassembly in the presence of Au particles and purification of BMV particles. This reassembly method is different from the synthesis method used by Douglas and Young because nanoparticles are simply added to the initial dissociated protein solution. Protein capsid precursors assemble together with the added nanoparticles through non-specific electrostatic interactions between the negative surface charge of the nanoparticle and the positively charged interior surface of the virus cavity. Although the yield of entrapment is inferior to the synthesis, the reassembly method can be applicable to a broad class of charged nanoparticles of arbitrary complexity.

For biomedical purposes, a key question for both methodologies is how would the replacement of the nucleic acid core by a nanoparticle interfere with the structural and functional characteristics of the native capsid? With the reassembly method, we need to conclusively demonstrate that a closed shell was formed and not an amorphous protein coating of the Au nanoparticles. In this work, we demonstrate that the formation of a closed shell does indeed occur and that the shell/core interactions can be tuned using different coatings on the nanoparticle core.

RESEARCH ARTICLE

2. EXPERIMENTAL DETAILS

Brome Mosaic Virus (BMV) is a model small icosahedral virus that infects a vast range of Poaceae species.[11] The native form is composed of 180 identical proteins of 20 kDa, which form pentameric or hexameric subunits. The ~28 nm diameter BMV capsid is most stable at low to moderate ionic strength buffers with pH below 5.0, but experiences a profound structural transition when the pH is increased from 5 to 7. In the presence of Mg^{2+}, which helps stabilizing the capsid at pH levels close to neutrality, reversible expansion occurs without dissociation. At pH 7.5 or higher, and ionic strength higher than 0.5 M, the capsid dissociates and the viral RNA precipitates. Upon reestablishment of low pH and ionic strength, reassociation occurs. The crystallographic structure of BMV is known from X-ray diffraction on intact virus crystals.[12] Bromovirus capsids have an arginine-rich motif on the inner surface that is juxtaposed to, but not interpenetrated by the negatively charged RNA. The nonspecific association between the negatively charged core and the positively charged inner capsid surface, and the dense positive charge of the internal surface make BMV an appropriate system to introduce functionalized nanoparticles inside the capsid.

The experimental procedure for encapsidation of carboxylated Au particles has been described elsewhere.[9] In brief, Au particles with tunable average diameters ranging between 3 and 20 nm (relative standard deviation 5–8%) at 10^{12}–10^{14} particles/ml are prepared by the Turkevitch method.[13] TEM and surface plasmon resonance spectroscopy are used to characterize the colloidal suspensions. The Au particles and the coat protein suspension solution are then mixed together and assembled by dialysis against the reassociation buffer: 50 mM NaOAc, pH 5.0, 100 mM NaCl, 0.2 mM PMSF for 10 hrs at 4 °C. Since the reassociation buffer has high ionic strength and low pH, which may favor aggregation, we have monitored the changes in the surface plasmon spectrum of the gold colloid as a function of the buffer pH and ionic strength to assess the extent of aggregation. We came to the conclusion that although partial aggregation does occur, most particles remained isolated over times and conditions typical for the virus reassembly experiment. We have also noticed that the addition of protein tends to stabilize the particles: bare citrate-coated gold will aggregates in the reassembly buffer at a significantly faster rate than in the presence of protein for the same buffer. In these conditions, dimers and trimers of particles, at quasi-equilibrium with single particles, have been found to dominate the aggregate distribution.[14] Density gradient centrifugation in sucrose at 50,000 rpm for 120 min at 4 °C followed by gel filtration through a G-50 column are employed to purify the intact capsid. This methodology does not separate Au-encapsulating capsids from empty capsids, but does remove the unassociated Au particles and capsid protein. The pellet contains enough Au particles to exhibit the characteristic pink coloration due to the surface plasmon resonance in Au.

3. RESULTS AND DISCUSSION

The TEM images on which our analysis is based, are projection maps of the sample density and cannot easily distinguish a Au particle laying on top of a capsid or one that is encapsidated. In support of the encapsidation, attempts of functionalization with swollen but not dissociated capsids failed.[9] This indicates that, for functionalization, access to and interaction with the internal surface of the capsid precursor is necessary and the TEM-observed Au particles are inside the capsid. Nonetheless, we seek a

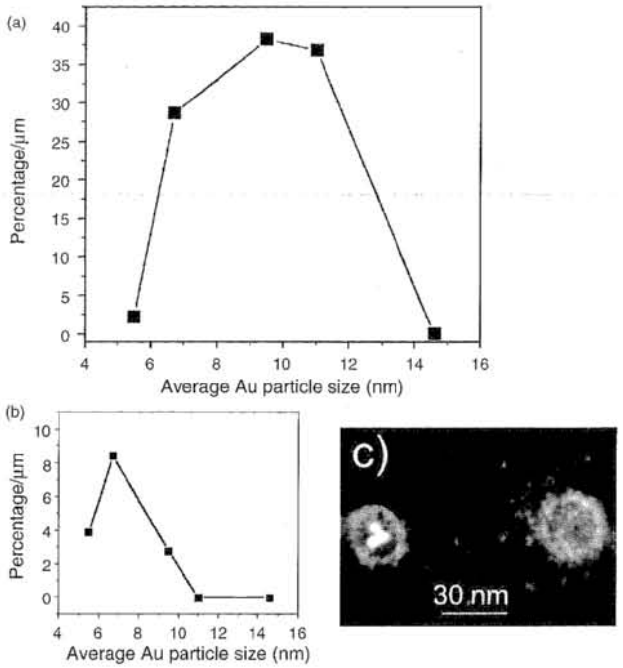

Fig. 1. (a) Percentage of Au-encapsulating capsids from the total number of capsids formed, normalized to the initial Au particle concentration as a function of the Au particle size. The cut-off in the size of the incorporable particles (~15 nm) dismisses the hypothesis of an amorphous capsid protein build-up. (b) For multiple encapsulated Au particles (here, triplets), the cut-off size is smaller than for single particles as one would expect from a volume restriction argument. (c) TEM micrograph illustrating an encapsidated 4 nm Au particle trimer and an empty viral capsid.

more direct demonstration that the capsid is encapsidating the Au particles. We predict that the specific encapsidation of Au would be limited by the inner diameter of the viral capsid. On the other hand, if there is non-specific adsorption of the capsid subunits onto Au cores, then one would expect an increase in the size of the complex as a function of the Au particle diameter.

We have therefore analyzed the variation of the TEM-measured external diameter of the Au/BMV particle as a function of the encapsidated Au particle size. Figure 1 shows a plot of the fraction of capsids containing Au particles.

Note that the percentage has been normalized to the initial concentration of Au particles. This way, we are able to compare the *relative* expectation ratio of incorporation per Au particle for different particle sizes. Typical *absolute* yields of incorporation are 1%.

Each data point in Figure 1 is the result of statistics over more than 2000 viral capsids. A cutoff diameter for the Au particles exists somewhere between 13 and 15 nm, which fits within the inner diameter of the BMV capsid of 18 nm. These results suggest that protein–protein interactions constrain the formation of the Au-functionalized capsid. Furthermore, the existence of a cut-off size brings additional support to the idea that the particles are inside the capsid since nonspecific attachment to the outside of

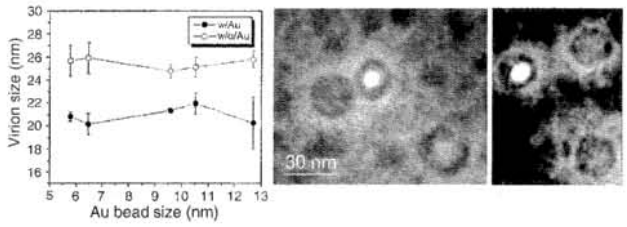

Fig. 2. Plot of the Au-encapsulating and empty capsid sizes as a function of the diameter of the Au particles used for the assembly assay and representative TEM micrographs of capsids incorporating 6.7 nm (middle) and 9.5 nm (right) diameter Au particles.

the capsid should not depend on a specific diameter of the Au particles.

It is interesting to note that Au particles smaller than ~6 nm have a significantly smaller yield of incorporation than larger particles of 8–10 nm. We do not have an explanation for this observation at this time. Assuming that the charge is uniformly distributed over the particle surface, we speculate that larger areas for electrostatic interaction, as long as it is within the packaging constraint, may actually favor the protein self-assembly process or result in a more stable particle. It has been suggested, for example, that the nucleation step for the capsid growth is the formation of a pentamer.[15] Particle cores smaller than the footprint of such a pentamer (~4 nm) could be poor supports for its formation.

The size of the viral capsid is another parameter providing insight on the characteristics of the Au/BMV association. Figure 2 shows the variation of the average capsid diameter with the encapsidated Au particle average diameter. We observed that, within the error range of our experiment, the capsid diameter does not vary with the Au core diameter and that the average Au-functionalized capsid diameter is smaller than the native BMV capsid diameter.

The TEM analysis requires introduction of the virus sample in vacuum. In solution, BMV viruses have an average diameter of 28 nm.[12] However, TEM micrographs of intact viral particles under vacuum yield an average particle diameter of ~26 nm.[16] This is consistent with the observation by Cuillel et al. that capsids contract by 10% upon dehydration for electron microscopy.[17] The average size of the Au-functionalized BMV is 21.5 nm, or ~24 nm for a hydrated particle, which indicates a different interaction between the citrate-coated Au core and the capsid than between the native RNA core and the capsid.

The fact that the Au-functionalized capsid diameter does not vary with the size of the Au core indicates that a fixed number of protein subunits form the capsid. The number of protein units in the Au-functionalized capsid is probably lower than the 180 necessary to build the native virion. The smaller capsid thus may correspond to a shift in the free energy minimum of the quasi-spherical structure due to a change in the spontaneous curvature parameter,[18] which was first proposed by Caspar and Klug as the main thermodynamic control parameter for the capsid size.[19]

However, further experiments able to provide structural information are needed to address this point.

It is interesting to calculate the inner cavity space corresponding to the dehydrated Au-BMV particles of 21.5 nm. The thickness of the hydrated capsid shell determined by crystallographic studies is 5.3 nm. The dehydrated protein shell would then correspond to ~4.8 nm. The maximum inner cavity diameter of the dehydrated intact virus is then approximately 16.7 nm. Hence, the experimental upper limit of 14.5 nm in the size of the incorporable Au particles is probably corresponding to the totality of available space inside the smaller capsid.

The fact that we find a capsid with a different diameter, and likely a lower number of subunits, than the native virion is not surprising. An alternative BMV capsid of 120 subunits that contained a messenger RNA rather than a viral genomic RNA was previously reported.[20] The alternative structure is approximately 10% smaller than the mature BMV virions. This fact suggests that even though the Au particles have been functionalized with negative charges, they are poor mimics for the viral RNA and cause the capsid protein to undergo an alternative assembly process. Consistent with this, there are additional signals within the viral RNAs that are needed for viral capsid assembly in the virus-infected cells.[21, 22]

In an attempt to reconstruct particles that better resemble mature BMV particles, we designed a DNA oligonucleotide that contained the equivalent of the high affinity capsid-binding site required for BMV encapsidation. DNA, rather than the more labile RNA of the BMV genome is used to increase the ease of handling. The oligonucleotides were synthesized with a di-biotin linker at its 5′ terminus and used to coat 5 nm Au particles that have been modified to have 2 to 3 avidin molecules per particle.

In vitro viral capsid assembly reactions using the DNA-coated Au particles lead to: (a) absence of incorporation events of multiple Au particles in the same capsid, (b) a two to three-fold increase in the yield of virus-like particles, and (c) dehydrated capsids that are now ~26 nm in diameter, Figure 3. The first aspect can be explained by a better stability of the Au particle suspension when DNA-stabilized colloids are used instead of citrate-stabilized colloids. As opposed to DNA-coated particles, for citrate-coated Au particles, dimers and trimers may be present in a metastable equilibrium with separated particles at the pH values used in this work as seen by surface plasmon resonance spectroscopy. The better yield of incorporation and the increase in size can be understood if we assume that the core-capsid interactions have changed, becoming in this case more similar to those present in normal viruses.

The differences between citrate-coated and DNA-coated particles have been addressed here for only one DNA sequence. Experiments testing the importance of the specific DNA sequence for the capsid self-assembly by using different oligonucleotides are on their way.

The optical density of the Au-DNA capsid sample is sufficiently high to allow subtracting the Raleigh scattering contribution from empty particles (Fig. 4(b)), and remain with the surface plasmon contribution from Au-containing particles, which then can be used to calculate the ratio between the Au-containing and empty BMV particles, as illustrated in Figure 4. Using this procedure, we found that the surface plasmon peak of DNA-coated Au shifts from 519.0 ± 0.5 nm to 522.0 ± 0.5 nm upon incorporation. This can be interpreted as due to the higher index of refraction of the protein coat than the initial solvent layer surrounding the DNA-coated particles.[23]

To further prove that the relatively large Au/Avidin/Biotin/DNA complex forms the core of the viral capsid, we tested the permeability of the capsid to fluorescent molecules that would be quenched by binding to the Au core. Figure 5 shows a comparison between the kinetics of the fluorescence quenching of biotinylated fluorescein and dextran-conjugates by encapsidated and free Au particles in solution. The two fluorescent markers have been chosen because they are based on the same chromophore but have very different sizes (647 MW and 10000 MW, respectively). Figure 5 shows that for both fluorescein and dextran rapid quenching occurs when the Au particles are free in solution. The concentration of free Au has been

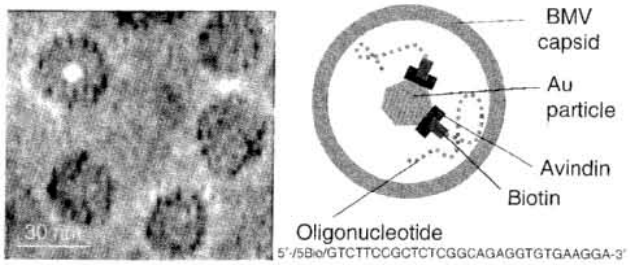

Fig. 3. Capids with DNA-coated Au cores are close to the size of the native virion. The synthetic DNA nucleotide sequence used in these experiments mimics an RNA motif that participates in BMV packaging.[21]

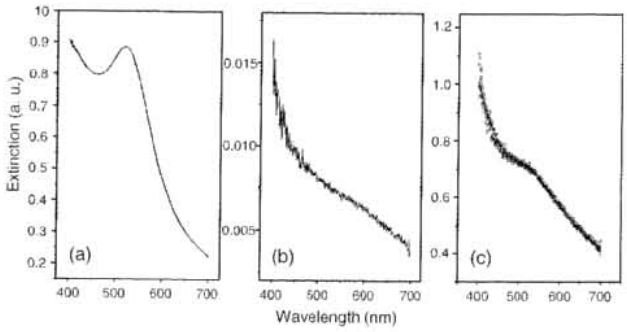

Fig. 4. Spectral extinction characteristics of DNA-coated gold particles. (a) The surface plasmon peak at 519 nm characterizing initial DNA-coated gold particles. (b) Spectral extinction due to empty BMV capsids. (c) A linear combination of the spectra in (a) and (b) (dots) is used to fit the experimental extinction spectrum of the DNA/Au/BMV solution (red line). The coefficients of the linear combination can be used for quantitative determinations of the relative concentrations of Au-containing and empty virions.

RESEARCH ARTICLE

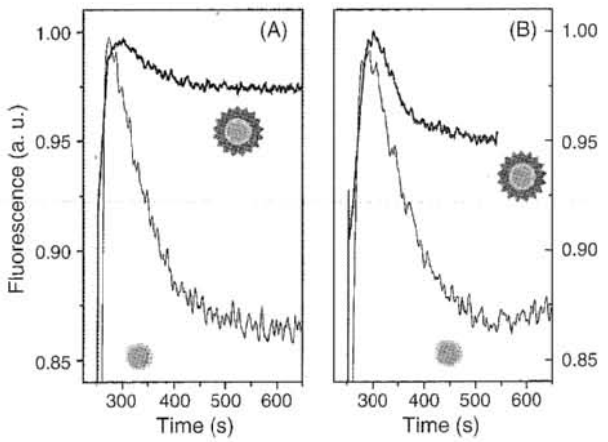

Fig. 5. (A) Dextran conjugate fluorescence quenching by free, avidin/biotin/DNA-coated Au particles in solution (black line) and by encapsidated avidin/biotin/DNA-coated Au particles (blue line). (B) Fluorescence quenching of fluorescein by free, avidin/biotin/DNA-coated Au particles in solution (black line) and by encapsidated avidin/biotin/DNA-coated Au particles (red line).

adjusted to the same optical density as the amount of Au inside capsids.

The quenching was considerably slower for the encapsidated Au particles. Control experiments with only protein and fluorescent markers (no gold) have not yielded any measurable fluorescence quenching. This indicates that the capsid forms an effective diffusion barrier preventing quenching. The pore sizes of this diffusion barrier must be big enough to allow fluorescein to pass, but too small for dextran. The small initial drop in fluorescence in both cases is probably due to binding of the conjugate to fragmented Au/BMV particles, which occasionally can be observed by TEM, too. We note that, when quantitative, such fluorescence quenching experiments could be very useful to estimate in real time the pore size of capsid intermediates undergoing structural transitions. However, for these experiments to be possible, one would need: (a) a better Au particle incorporation yield, which would increase the sensitivity of the measurement by a more effective quenching, and (b) a series of fluorescent markers with different sizes.

4. CONCLUSIONS

In conclusion, we have shown that reassociation could be used to package foreign material in the core of the virus capsid. A major result of this study is that the protein coat is achieved by closed shell formation, which leaves open the possibility that some of the functional characteristics of the native virus coat are preserved. Furthermore, different capsid structures could be fine-tuned based on the functionalities on the Au surface. We note that each of the 21.5 and the 26 nm virus-like particles could have desirable, but distinct properties. These results also indicate that we should be able to manipulate the Au surface to achieve more efficient incorporation and closer similarity with the wild type virions. Finally, the integrity of the viral coat has been qualitatively tested using a fluorescence-quenching assay based on the permeability of the virus capsid to different fluorescent conjugates. The encapsidation method described here is likely to be applicable to other materials of biomedical and technological interest, but further work is needed to assess the degree in which the functional characteristics of the capsid are affected upon the replacement of the nucleic acid with a synthetic core.

References and Notes

1. D. H. Bamford, R. J. C. Gilbert, J. M. Grimes, and D. I. Stuart, *Current Opinion in Structural Biology* 11, 107 **(2001)**.
2. R. Lata, J. F. Conway, N. Q. Cheng, R. L. Duda, R. W. Hendrix, W. R. Wikoff, J. E. Johnson, H. Tsuruta, and A. C. Steven, *Cell* 100, 253 **(2000)**.
3. A. Callaway, D. Giesman-Cookmeyer, E. T. Gillock, T. L. Sit, and S. A. Lommel, *Ann. Rev. Phytopathology* 39, 419 **(2001)**.
4. J. B. Bancroft, *Adv. Virus Res.* 16, 99 **(1970)**; K. W. Adolph and P. J. G. Butler, *Nature* 255, 737 **(1975)**; V. Percec, *Journal of Macromolecular Science-Pure and Applied Chemistry* A33, 1479 **(1996)**.
5. T. Douglas and M. Young, *Nature* 393, 152 **(1998)**.
6. Q. Wang, T. W. Lin, L. Tang, J. E. Johnson, and M. G. Finn, *Angewandte Chemie-International Edition* 41, 459 **(2002)**; T. Douglas, E. Strable, D. Willits, A. Aitouchen, M. Libera, and M. Young, *Adv. Mater.* 14, 415 **(2002)**; S. W. Lee, S. K. Lee, and A. M. Belcher, *Adv. Mater.* 15, 689 **(2003)**.
7. D. Bradley, *Pharmaceutical Science & Technology Today* 1, 146 **(1998)**.
8. M. Lakadamyali, M. J. Rust, H. P. Babcock, and X. W. Zhuang, *Proceedings of the National Academy of Sciences of the United States of America* 100, 9280 **(2003)**.
9. B. Dragnea, C. Chen, E. S. Kwak, B. Stein, and C. C. Kao, *J. Am. Chem. Soc.* 125, 6374 **(2003)**.
10. X. X. Zhao, J. M. Fox, N. H. Olson, T. S. Baker, and M. J. Young, *Virology* 207, 486 **(1995)**.
11. L. C. Lane, *CMI/AAB Descript. Plant Viruses* 180, 1 **(1977)**.
12. R. W. Lucas, S. B. Larson, and A. McPherson, *J. Mol. Biol.* 317, 95 **(2002)**.
13. J. Turkevitch, P. C. Stevenson, and J. Hillier, *Trans. Faraday Soc.* 11, 55 **(1951)**.
14. C. Cheng, B. Stein, C. Kao, and B. Dragnea, in preparation.
15. J. M. Johnson, D. A. Willits, M. J. Young, and A. Zlotnick, *J. Mol. Biol.* 335, 455 **(2004)**.
16. C. C. Kao and K. Sivakumaran, *Mol. Plant Path.* 1, 91 **(2000)**.
17. M. Cuillel, M. Zulauf, and B. Jacrot, *J. Mol. Biol.* 164, 589 **(1982)**.
18. R. F. Bruinsma, W. M. Gelbart, D. Reguera, J. Rudnick, and R. Zandi, *Phys. Rev. Lett.* 90 **(2003)**.
19. D. L. D. Caspar and A. Klug, *Cold Spring Harbor Symp. Quant. Biol.* 27, 1 **(1962)**.
20. M. A. Krol, N. H. Olson, J. Tate, J. E. Johnson, T. S. Baker, and P. Ahlquist, *Proceedings of the National Academy of Sciences of the United States of America* 96, 13650 **(1999)**.
21. T. A. Damayanti, S. Tsukaguchi, K. Mise, and T. Okuno, *J. Virol.* 77, 9979 **(2003)**.
22. Y. G. Choi, G. L. Grantham, and A. L. N. Rao, *Virology* 270, 377 **(2000)**.
23. A. C. Templeton, J. J. Pietron, R. W. Murray, and P. Mulvaney, *J. Phys. Chem. B* 104, 564 **(2000)**.

Received: 8 November 2004. Revised/Accepted: 8 March 2005.

RESEARCH ARTICLE